KSOE

Journal of Ocean Engineering and Technology 39(1), 82-91, February, 2025 eISSN 2287-6715
https://doi.org/10.26748/KSOE.2024.096

Original Research Article

Effects of Irregular Bathymetry on the Performance and Wake Characteristics of Tidal Stream Turbines: A Case Study of a Tidal Power Site

Ngome Mwero[1], Song Fu[2], Takafumi Inamitsu[3], Stephanie Ordonez-Sanchez[4], Benson Mwangi[5], Patxi Garcia-Novo[6], Cameron Johnstone[7] and Daisaku Sakaguchi[8]

[1]*Graduate Student, Graduate School of Integrated Science and Technology, Nagasaki University, Nagasaki, Japan.*
[2]*Researchh Associate, Department of Mechanical and Aerospace Engineering, University of Strathclyde, Glasgow, Scotland*
[3]*Graduate Student, Graduate School of Integrated Science and Technology, Nagasaki University, Nagasaki, Japan*
[4]*Lecturer, Department of Mechanical and Aerospace Engineering, University of Strathclyde, Glasgow, Scotland*
[5]*Lecturer, Department of Marine Engineering, Jomo Kenyatta University of Agriculture and Technology, Nairobi, Kenya*
[6]*Assistant Professor, Institute of Integrated Science and Technology, Nagasaki University, Nagasaki, Japan*
[7]*Professor, Department of Mechanical and Aerospace Engineering, University of Strathclyde, Glasgow, Scotland*
[8]*Professor, Institute of Integrated Science and Technology, Nagasaki University, Nagasaki, Japan*

KEYWORDS: Bathymetry, Wake recovery, Shear stress turbulent model, Tidal turbine, Computational fluid dynamics

ABSTRACT: *Tidal energy has emerged as a promising renewable energy source, with abundant marine resources available in many parts of the world. To exploit this resource efficiently, reliable and computationally efficient methods are required to analyze energy yields from tidal arrays in real sites worldwide. This paper investigates the impact of irregular-bathymetry seabed elements near a tidal turbine location on the turbine's performance and wake. A high-resolution three-dimensional bathymetry model was created, and full-scale unsteady simulations were performed using the ANSYS-Fluent computational fluid dynamics tool and the Shear Stress Turbulence (SST) model for two cases: one with the site bathymetry and one with a flat seabed. Compared to the flatbed case, the results show a 1.84% increase in the average turbine power output for the site-bathymetry case. A 4.1% increase in average wake recovery rate was observed near the hill-like seabed features from 3D to 7D downstream from the turbine, followed by 11% reduction in wake recovery rate over the bathymetry slope from 9D downstream from the turbine. The findings of this study highlight the implications of bathymetry-generated effects in optimal site selection and tidal energy farm design.*

1. Introduction

The ever-increasing global power demand and growing concerns about climate change have necessitated the rapid development of renewable energy sources as alternatives to conventional fossil fuels. To achieve this goal, Japan has embarked on an ambitious "Clean Energy Strategy" aimed at achieving carbon neutrality by 2050 and a 46% reduction in greenhouse gas (GHG) emissions by 2030 (Ozawa, et al., 2022). Recent geopolitical events have further undermined global energy security, underscoring the urgent need for dedicated investment and the development of renewable energy. Among other marine resources, tidal energy offers a desirable renewable energy option because of its high predictability and power density compared with wind energy (Khare and Bhuiyan, 2022).

Tidal turbines are the tidal energy-harvesting technology of choice for various configurations. Horizontal axis tidal turbines (HATTs) are preferred for power generation owing to their higher energy conversion efficiency and large self-starting torque (Bir et al., 2011; Yan et al., 2022), compared to other types. In addition to the tidal current speed, which directly translates to the amount of kinetic energy available for conversion to electricity (Ouro and Nishino, 2021), the presence of seabed elements near a tidal turbine location in irregular bathymetry has a pronounced effect on the performance and wake characteristics of the tidal turbine owing to the induced pressure

Received 14 November 2024, revised 22 January 2025, accepted 3 February 2025
Corresponding author Ngome Mwero: +81-702-797-3990, bb54524004@ms.nagasaki-u.ac.jp
This is a paper from the proceedings of 2024 Asian Offshore Wind, Wave, and Tidal Energy Conference held in Busan, Korea (Mwero et al., 2024).

ⓒ 2025, The Korean Society of Ocean Engineers
This is an open access article distributed under the terms of the creative commons attribution non-commercial license (http://creativecommons.org/licenses/by-nc/4.0) which permits unrestricted non-commercial use, distribution, and reproduction in any medium, provided the original work is properly cited.

gradients, particularly at shallow-depth sites where fast tidal currents are expected (Hurubi et al., 2023). These effects are of great significance in tidal stream energy farm design because the performance of downstream turbines (generated power and turbine loading) depends on the wake characteristics of the upstream turbines (Mercier et al., 2020). The wake of a tidal turbine is defined as the area of disturbed flow downstream of the turbine, which is usually characterized by a reduced flow speed and swirl with increased turbulence (Jump et al., 2020). Therefore, a faster wake dissipation is desired to restore the flow to its 'before turbine' condition, through a process called wake recovery.

Recently, several studies have been conducted to characterize the effects of wake-bathymetry interactions on tidal turbines. Ouro and Stoesser (2019) used a large eddy simulation (LES) to quantify the impact of bathymetry on the performance and structural loading of an HATT using the direct forcing immerse boundary (IB) method in Hydro3D to represent the irregular bathymetry. Their results revealed that dune-induced turbulence enhanced wake recovery compared with the flatbed case. Using the lattice Boltzmann method to represent irregular bathymetry conditions, Mercier and Guillou (2021) investigated the impact of seabed morphology on the hydrodynamic properties of the flow. They observed high spatial variability in turbulent kinetic energy (TKE) production, with high-TKE areas showing reduced flow velocity. Gaurier et al. (2020) further performed physical modelling of bathymetry-generated turbulence effects on turbine behavior using a wall-mounted cylinder in a flume tank to represent bathymetry variations and concluded that bathymetry-induced turbulence structures cause low-frequency velocity fluctuations, affecting turbine loading. Meanwhile, Chen et al. (2023) used flume bottom-mounted triangular prisms of varying sizes as bathymetry to study the effects of seabed topography on tidal stream turbine behavior. Their results showed an increased turbine output in the presence of a small seabed topography and vice versa with a larger seabed topography. Hurubi et al. (2023) used short ridges with varying streamwise lengths to mimic bathymetry variations. They observed that wake recovery was enhanced when the turbine was located upstream of the ridge compared to a flat channel, and the turbine experienced high fatigue loads when located downstream of the ridge. Ikhennicheu et al. (2019) used several obstacles to reproduce Alderney Race bathymetry variations and concluded that different obstacle shapes, combinations, and aspect ratios have a significant effect on the turbine wake and turbulent structures. More recently, Ouro et al. (2023) assessed the layout of a small tidal array deployed on the Shetland Islands (UK). They also concluded that the flow and bathymetry asymmetry caused different wake characteristics and interactions between turbine wakes in different rows.

The foregoing studies have demonstrated that bathymetry has a significant effect on turbine performance. However, most studies have used approximate structures, such as ridges and obstacles of various shapes and sizes, to represent irregular bathymetry and not the real fluctuating seabed. Therefore, the full extent of bathymetry-induced effects remains unclear. Therefore, a more detailed, full-scale flow and wake analysis is required, particularly for real turbine sites. This study aimed to further the existing research with a computational investigation of bathymetry effects on the wake characteristics of a tidal turbine installed in the Naru Strait, Nagasaki Prefecture, Japan. A high-resolution, full-scale three-dimensional (3D) model of the turbine installation site was used in this study, with the analysis focusing on the temporal velocity distribution, vorticity, and wake recovery within the study domain.

2. Methods

2.1 Turbine Site Description

The turbine site whose bathymetry is considered in this study was the Naru Strait in the Goto Islands, Nagasaki Prefecture, Japan, where the first tidal energy demonstration project in Japan was conducted in 2021 (Garcia-Novo et al., 2024). Naru Strait is one of the two channels (the other is Tanoura Strait) designated for tidal stream energy harvesting by the Government of Japan, among the four main channels formed by the five islands that constitute Goto (Waldman et al., 2017). The Goto Islands are characterized by narrow and relatively shallow channels and large water masses moving from the Pacific Ocean to the Sea of Japan and the Yellow Sea during flood tides and vice versa during ebb tides, generating strong tidal currents. Located between the Hisaka (west) and Naru (east) islands, Naru Strait is approximately 7 km long and 2 km wide, with a recorded vertically averaged maximum velocity of 3.1 m/s (Garcia-Novo et al., 2018). A map of the Goto Islands showing the turbine location in Naru Strait is shown in Fig. 1. The turbine location coordinates are 32°49′ 04.3″ N–128°54′ 40. 4″ E. The depth of the deepest point at the site is 50 m, and the mean water depth at the turbine location is 40 m, with a turbine hub height of 15 m above the seabed (Ministry of Environment, Government of Japan, n.d.).

2.2 Computational Setup

A high-resolution 3D bathymetry model of the domain of interest in the Naru Strait around the turbine location was created using topological map data, as shown in Fig. 2. The bathymetry is characterized by an elongated ridge with small undulating dunes near the turbine location. The ridge is raised approximately 10 m from the lowest point in the domain and is separated from the hill to the left by a 10-m-deep valley. A steep slope exists at the end of the ridge towards the outlet end of the domain. The computational domain size was 540 × 360 m, oriented parallel to the dominant flow direction of the accelerating ebb tides, as determined by Garcia-Novo et al. (2024, 2018). The water column height in the domain varied from 50 m at the lowest point to 35 m at the highest point. The analysis domain is shown in Fig. 3, which presents the seabed, inlet, outlet, and top and side boundaries. Three cases were considered in this study: a real bathymetry with a turbine (Case 1), a flatbed with a turbine (Case 2), and a real bathymetry without a turbine (Case 3). A constant water

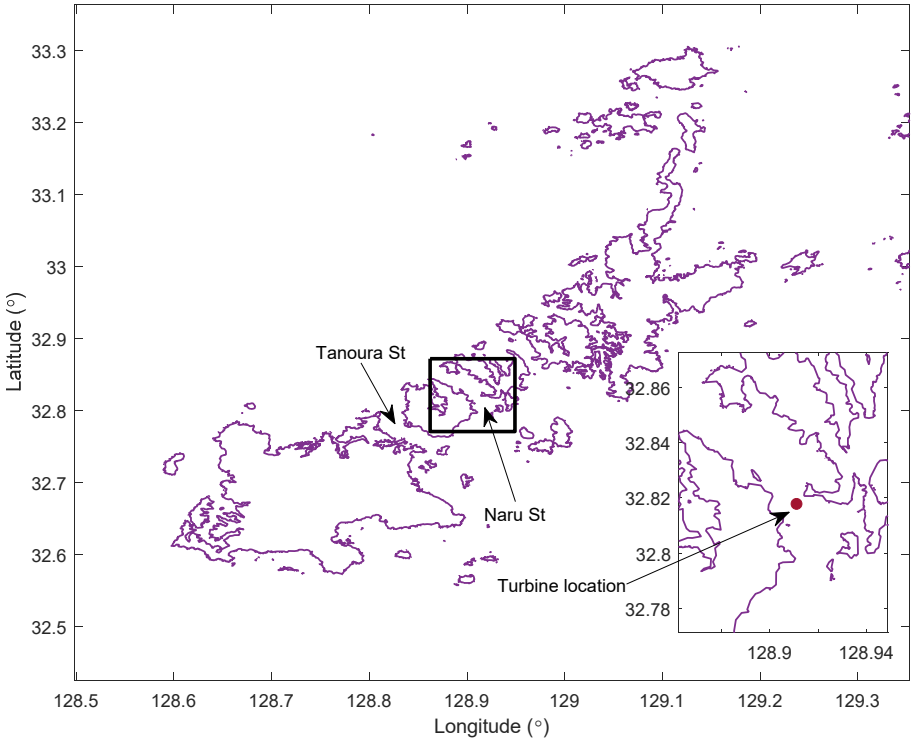

Fig. 1 Map of the Goto Islands showing the turbine location in the Naru Strait (Garcia-Novo et al., 2018)

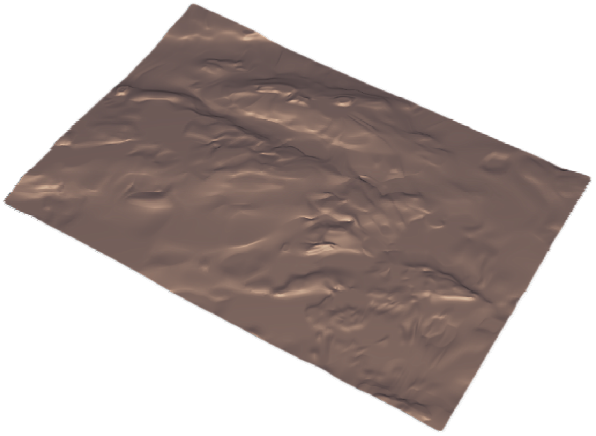

Fig. 2 Three-dimensional bathymetry model within the analysis domain

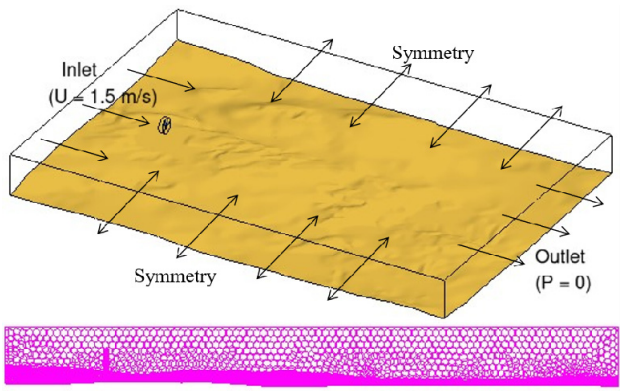

Fig. 3 Analysis domain showing the seabed, inlet, outlet, and top and side boundaries

depth of 40 m, which was similar to the depth at the turbine location, was used in Case 2. The ANSYS-Fluent computational fluid dynamics code was used to perform the 3D viscous flow analysis of the turbine using the k-ω Shear Stress Turbulence (SST) Reynolds averaged Navier-Stokes (RANS) model. Owing to tidal currents and irregular bathymetry interactions, turbulent flow exists in the water column near the seabed. Therefore, seabed boundary layers require a turbulence model to account for bathymetry roughness (Launder and Spalding, 1974). The k-ω SST model integrates the accuracy of the k-ω model in the boundary layer region close to the wall and the k-ϵ model in the free stream, using a blending function. Flow separation under adverse pressure gradients (APGs) and turbulent oscillating boundary layer flows over rough bottoms can be precisely predicted using this model (Holmedal et al., 2013). The inlet boundary was located 5D upstream of the turbine and the outlet 25D downstream of the turbine. The seabed, flatbed, turbine blades, and hub were modelled as walls, whereas the sides and upper boundaries were assigned symmetry boundary conditions. Standard inflow-outflow boundary conditions were used for the inlet and outlet, with the inlet velocity taken as the depth-averaged flow velocity, U_0 = 1.5 m/s, and the outlet pressure P was set to 0 Pa. The domain was discretized using ANSYS Fluent meshing as a watertight geometry with no voids and differentiated local sizing. A polyhexcore unstructured mesh that flexibly combines polyhedral and hexahedral elements was used. The mesh consisted of 25.4 million cells. An unsteady flow analysis was conducted, and the solution was run for 960 time steps, with each time step fixed at 0.5 s. The turbine rotation speed was set according to the specifications of the turbine used in the demonstration project in the Naru Strait for an

Table 1 Turbine design specifications (Allmark et al., 2020)

Blade profile	Wortman FX63 − 137
Max chord length	109.6 mm at a hub-to-rotor radius ratio of r/R = 0.382
Blade length	385 mm
Blade twist	19°
Hub diameter/Rotor diameter	0.14

Note: r = hub radius; R = Rotor radius

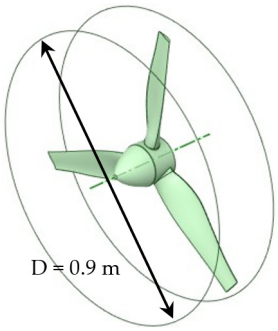

Fig. 4 Original turbine used for analysis

Table 2 Simulation conditions

Solver	ANNSYS Fluent
Method	Simple
Solution type	Unsteady
Model	k-ω SST Model
Inlet velocity, U_0	1.5 m/s
Outlet pressure, P	0 Pa
Runtime	960 steps @ 0.5-s time steps

inlet current velocity of 1.5 m/s. The original turbine adopted for the analysis is shown in Fig. 4, and its description is presented in Table 1. The simulation conditions are listed in Table 2.

2.3 Reynold Number Scalability

The turbine used for analysis is a scaled-up model of the 0.9-m-diameter HATT with a Wortmann FX 63-137 airfoil profile, which was designed in collaboration between the University of Strathclyde and Cardiff University through the Dylotta project. This HATT was tested by Allmark et al. (2020, 2021). The turbine was scaled up to 18 m, a diameter similar to that of the 0.5-MW turbine deployed in the demonstration project in Naru Strait. To ensure similarity in terms of flow characteristics between the original and scaled-up turbines, dynamic similarity should be maintained. However, while the original turbine was tested in a flume tank, where the Reynolds number (Re) and other flow parameters could be readily controlled, the scaled-up turbine operated under varying turbulent flow conditions owing to the irregular bathymetry. In this study, the characteristic curves of the non-dimensional performance parameters (power and thrust coefficients) were used to assess the Re-independence of the scaled-up turbine, as proposed by Allmark et al. (2019) and Ordonez-Sanchez et al. (2019). The instantaneous turbine torque (T), thrust (τ), power coefficient (C_P), and thrust coefficient (C_T) at the tip speed ratio (λ) resulting from Eq. (1) for the flow velocity (U) and rotation speed (ω), were used in this study. C_P and C_T are expressed as in Eqs. (2) and (3), respectively, where A is the flow area and ρ is the water density.

$$\lambda = \frac{\omega R}{U} \tag{1}$$

$$C_P = \frac{T\omega}{0.5\rho U^3 A} \tag{2}$$

$$C_T = \frac{\tau}{0.5\rho U^2 A} \tag{3}$$

3. Results

A comparison of the turbine wake characteristics and performance in the presence of bathymetry (Case 1) and over flatbed (Case 2) is presented in this section. The bathymetry effect on the flow hydrodynamics at the site without a turbine (Case 3) is also presented.

3.1 Turbine Performance and Scalability

The turbine torque and thrust output time series are shown in Fig. 5, and the average values of the performance results are listed in Table 3.

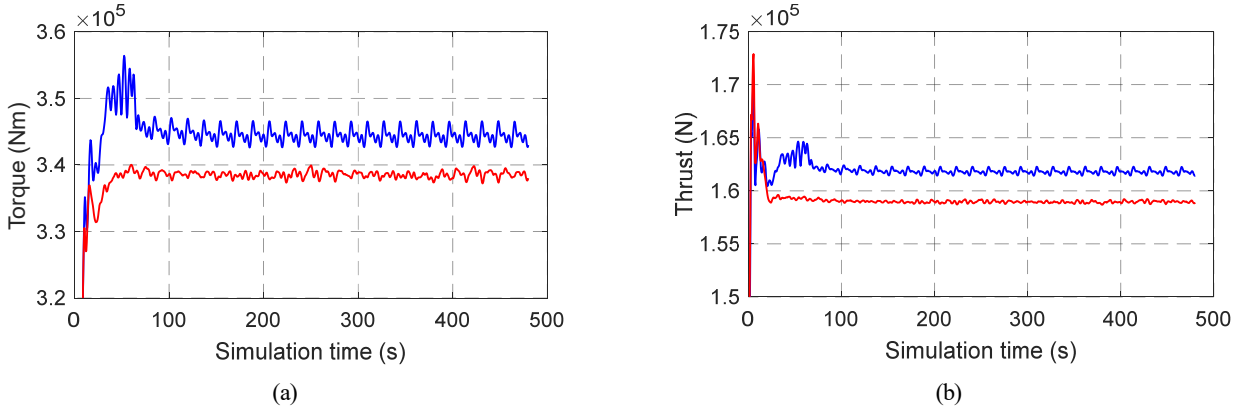

Fig. 5 Turbine (a) torque and (b) thrust variations for Cases 1 (blue) and 2 (red)

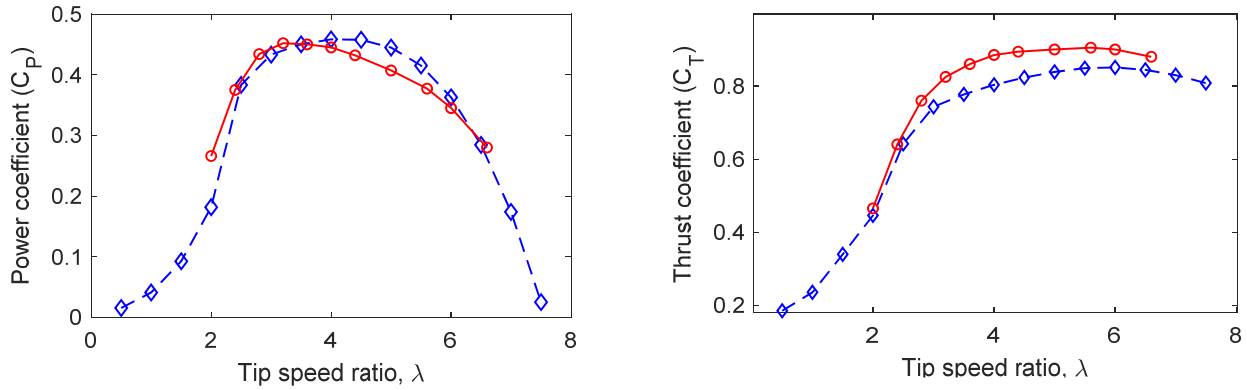

(a) (b)

Fig. 6 Comparison of the (a) power and (b) thrust coefficients between the original 0.9-m-diameter (red) and scaled up 18-m (blue) turbines used in the current analysis

Table 3 Turbine performance comparison

	Torque (kN·m)	Thrust (kN)	C_P	C_T
Case 1	345.20	162.09	0.293	0.567
Case 2	338.96	159.17	0.287	0.557
Original turbine	-	-	0.305	0.540

The results show that the turbine power output in the presence of irregular bathymetry was 1.84% higher than that in the flatbed case. Bathymetry contributes to improved turbine power, although with a 1.73% increase in thrust loading. Periodic fluctuations were also observed in the turbine torque and thrust outputs. The torque fluctuations in Case 1 have amplitudes 1.9× larger than those in Case 2. A similar observation was made for thrust fluctuation, but with smaller amplitudes. In both cases, the fluctuations occurred at a frequency consistent with the turbine rotational speed. This not only implies increased turbulence but also increased fatigue loading on the turbine blades in the presence of bathymetry. However, these effects require further research.

Fig. 6 shows a comparison of the power and thrust coefficient curves of the original 0.9-m-diameter and scaled-up 18-m-diameter turbines. The original turbine was tested at a tip ratio range of $\lambda = 2$–7. Table 3 summarizes the turbine performance comparison. The results show that at a tip speed ratio corresponding to the demonstration project specifications, differences of 3.93% and 4.76% in the C_P and C_T values, respectively, were observed between the original and scaled-up turbines. The close correlation between the non-dimensional performance curves indicates good scalability and Re independence for the scaled-up turbine. However, the turbine does not operate at its peak efficiency, which occurs at approximately $\lambda = 4$. Therefore, further research should be conducted under these conditions.

3.2 Wake Characteristics

The streamwise velocity distribution and wake development behind the turbine in Cases 1 and 2 are shown in Fig. 7. A clear distinction exists between the wake profiles for the bathymetry and flatbed cases. The turbine in the real bathymetry case exhibited a smaller reverse-flow area compared to the flatbed case. The turbine receives an accelerated flow from the upstream hill, which induces a favorable pressure gradient. The flow was accelerated by up to 5.2% of the inlet velocity and was maintained over the ridge. Then, a reduction in flow velocity occurred, coinciding with the slope in bathymetry 7D downstream of the turbine. There is a vertical wake expansion towards the seabed and water surface owing to flow separation. This phenomenon is more pronounced near the end of the domain, where the largest depth exists, experiencing up to 8.6% reduction in flow velocity along the turbine axis and 15% velocity reduction at the deepest point of the domain.

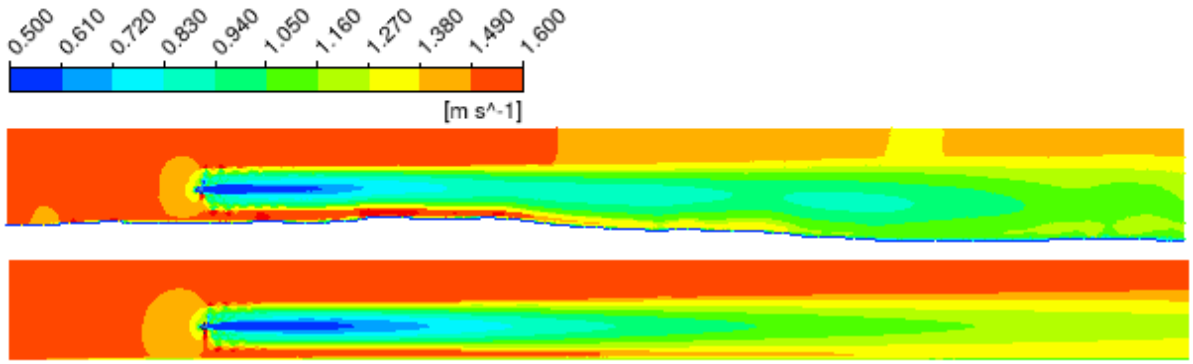

(a)

(b)

Fig. 7 Streamwise velocity contours over a vertical plane through the hub axis for Cases (a) 1 and (b) 2

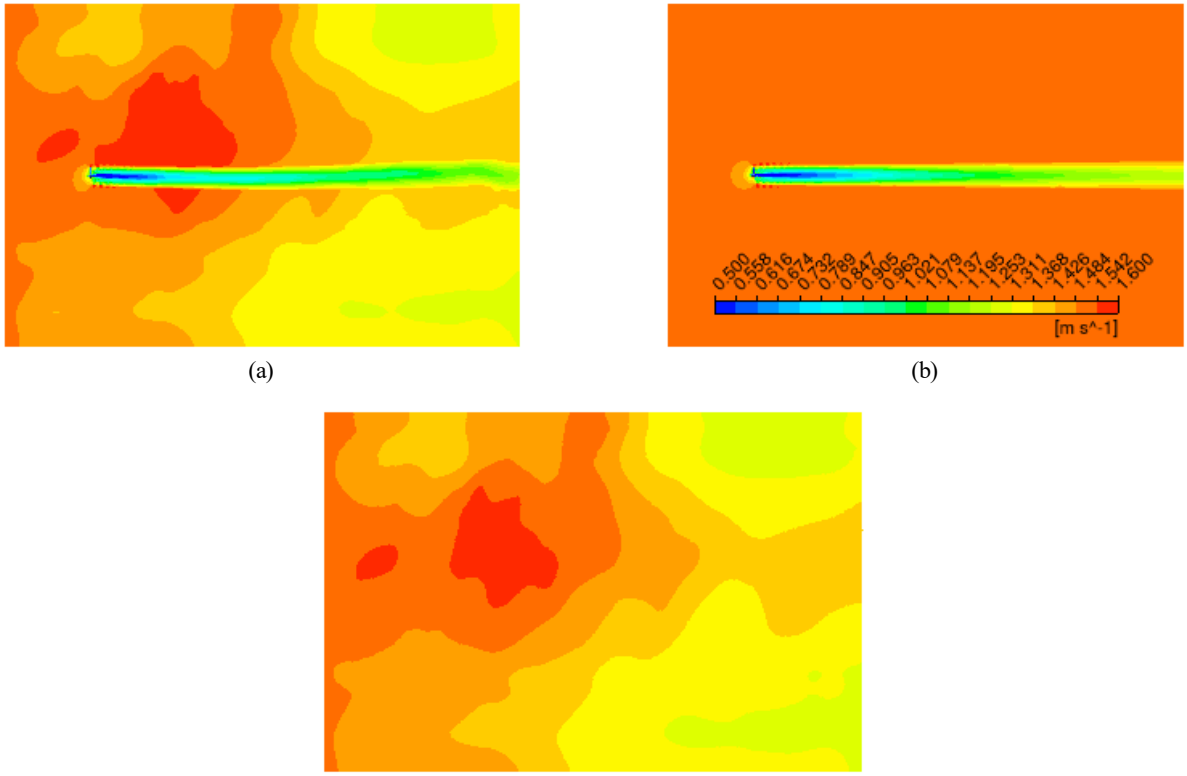

(a) (b)

(c)

Fig. 8 Streamwise velocity contours over a horizontal plane through the hub axis showing the turbine wake meandering for Cases (a) 1, (b) 2, and (c) 3

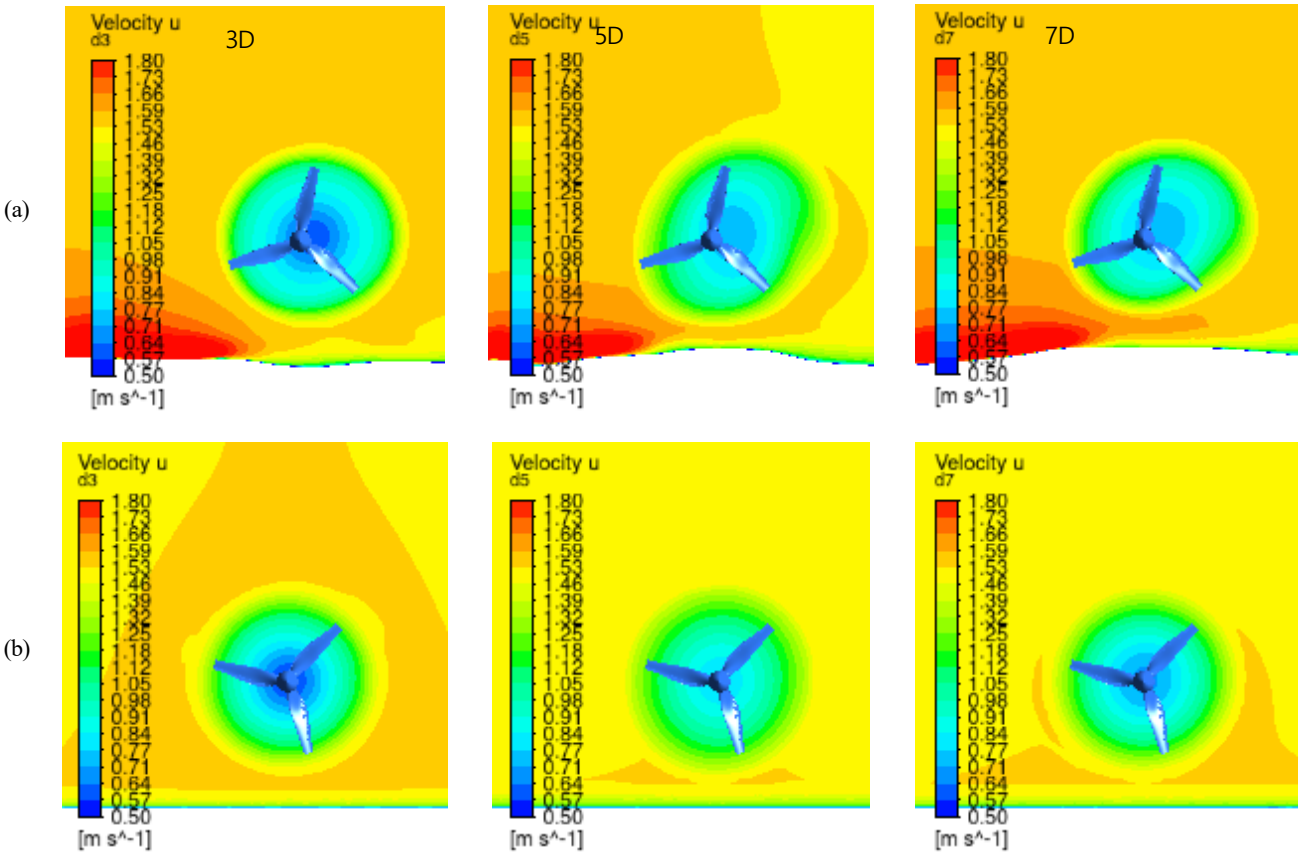

(a)

(b)

Fig. 9 Streamwise velocity contours over planes perpendicular to the flow direction, showing a comparison of the wake shifting phenomena at selected downstream positions for Cases (a) 1 and (b) 2

Fig. 8 shows the streamwise velocity field over the horizontal plane at the turbine hub height. The contours in Case 3 show that the seabed topology causes high spatial variability in the average flow velocity, even without the turbine. The turbine in Case 1 operates in a complex mix of favorable and adverse pressure gradients that not only cause significant velocity distribution variations but also contribute to the wake meandering and shifting phenomena shown in Figs. 8 and 9. These effects can result in notable variations in the power output and loading on a tidal farm's downstream turbines (Brugger et al., 2022). However, the turbine in Case 2 operates in a zero-pressure gradient and therefore experiences negligible wake-meandering and shifting effects. Furthermore, the seabed features caused faster vortex dissipation in Case 1 owing to the scattering of the vortex structures, as shown in Fig. 10. The streamwise vorticity magnitude distribution in the wake-recovery zone behind the turbine is illustrated in Fig. 11. As expected, stronger vortices were formed in the near-wake zone, followed by an initially faster dissipation. Case 1 exhibited 16.1% faster average vortex dissipation than Case 2, although comparatively

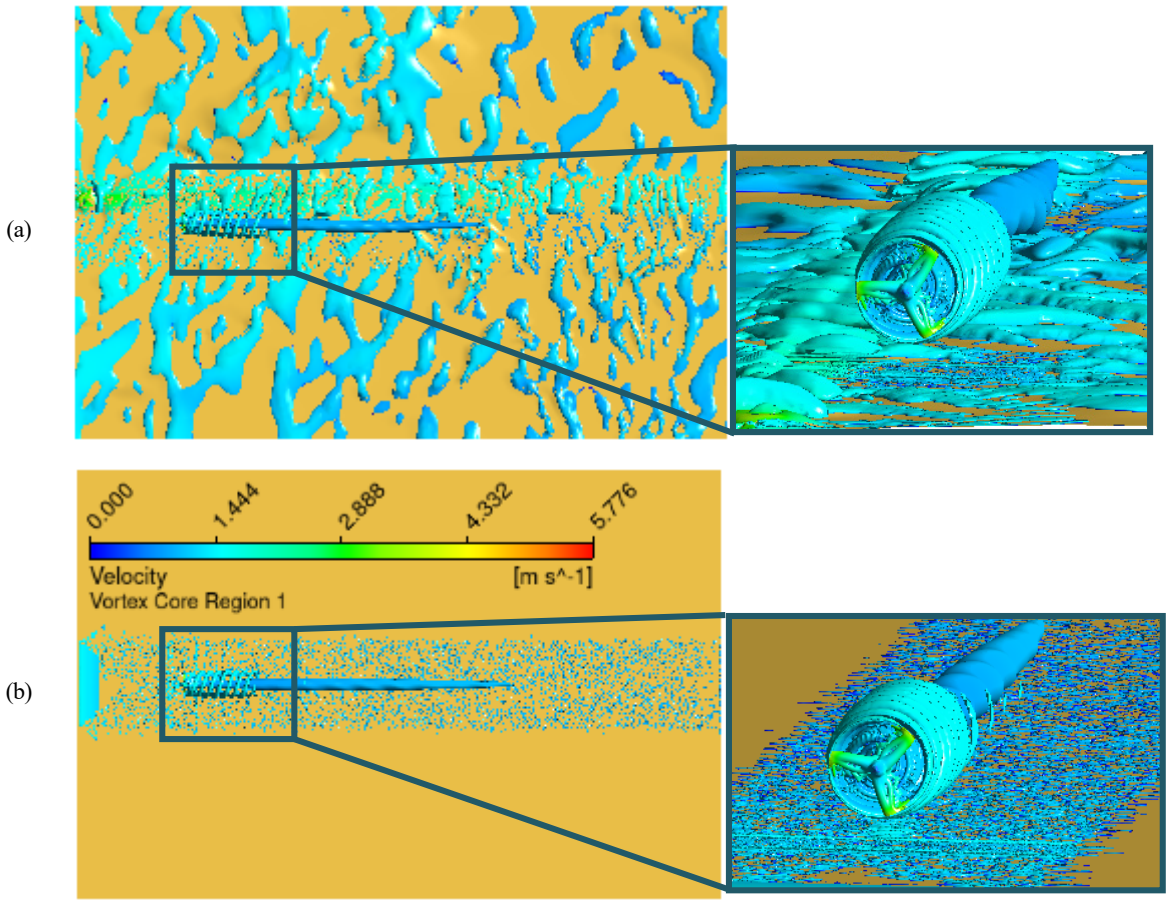

Fig. 10 Comparison of the vortex core region measured by the Q-criterion showing the blade tip vortex development and the dissipation and scattering of vortex structures by the seabed features for Cases (a) 1 and (b) 2

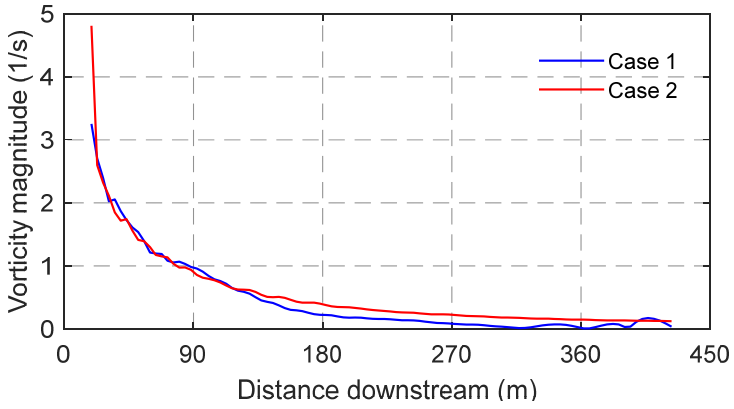

Fig. 11 Streamwise vorticity magnitude distribution in the wake-recovery zone behind the turbine

stronger fluctuating vortices were observed in the far-wake zone. This could also have a negative effect on the downstream turbines in a tidal array; therefore, further research is required.

3.3 Velocity Deficit and Wake Recovery

To analyze and quantify the wake recovery, the velocity deficit (U/U_o) was used in this study. This is defined as the non-dimensional ratio of the flow velocity at a downstream location U, to the inlet flow velocity U_o. The streamwise U/U_o vertical profiles are shown in Fig. 12. A 4.1% increase in the average wake recovery rate was observed over the elongated ridge-like seabed feature between 3D and 7D downstream of the turbine, where the flow was accelerated owing to the bathymetry-induced favorable pressure gradient (FPG). By contrast, the drastic slope in the bathymetry from 9D downstream of the turbine to the end of the domain caused a reduction in the average wake recovery of approximately 11.1% compared to the flatbed case. The seabed slope induces APGs that decelerate the flow. The profile for Case 3 shows that the flow was accelerated upstream of the turbine by the small hill feature and over the ridge-like feature. However, negative flow recovery was observed over the bathymetry slope, even without the turbine. Fig. 13 shows the mean pressure distribution over the vertical plane through the turbine axis. It can be observed that the wake of the turbine is subjected to varying pressure fields because of the seabed topology that induces FPGs and APGs, as indicated by the purple circles, which cause enhanced and slow wake-recovery phases, respectively.

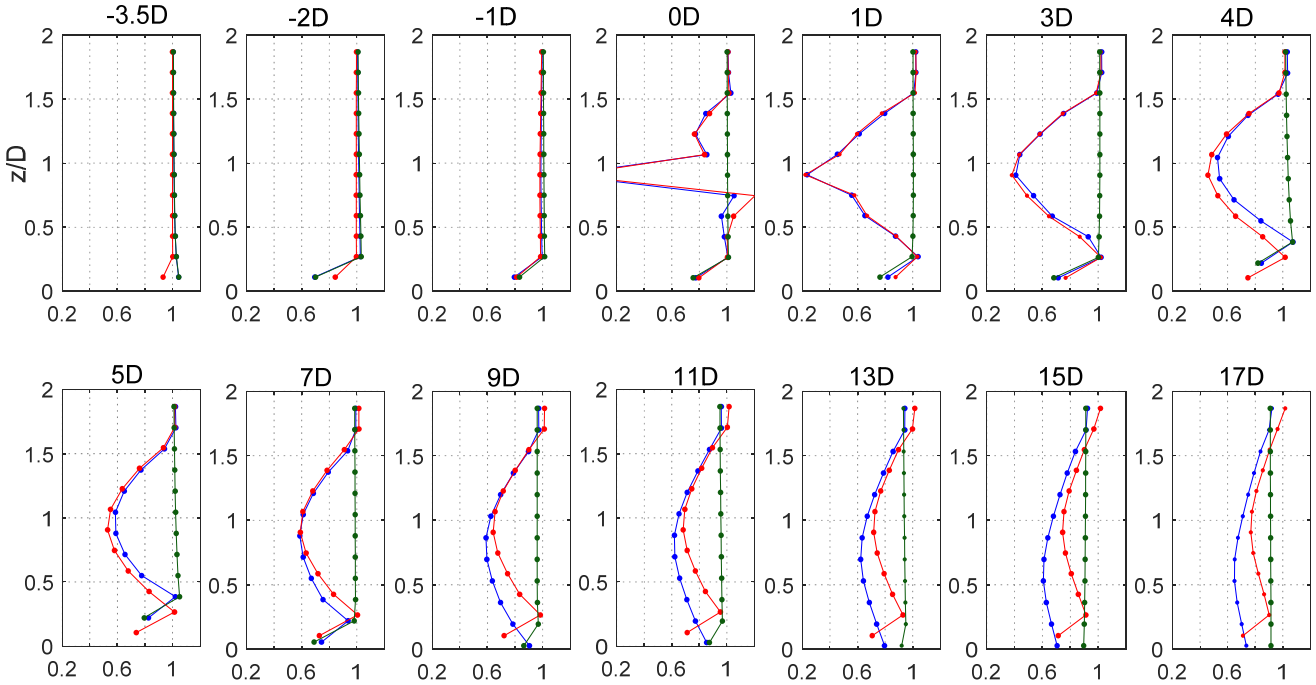

Fig. 12 Vertical profile of the streamwise mean velocity deficit showing the turbine wake recovery at different downstream locations for Cases 1 (blue), 2 (red), and 3 (green)

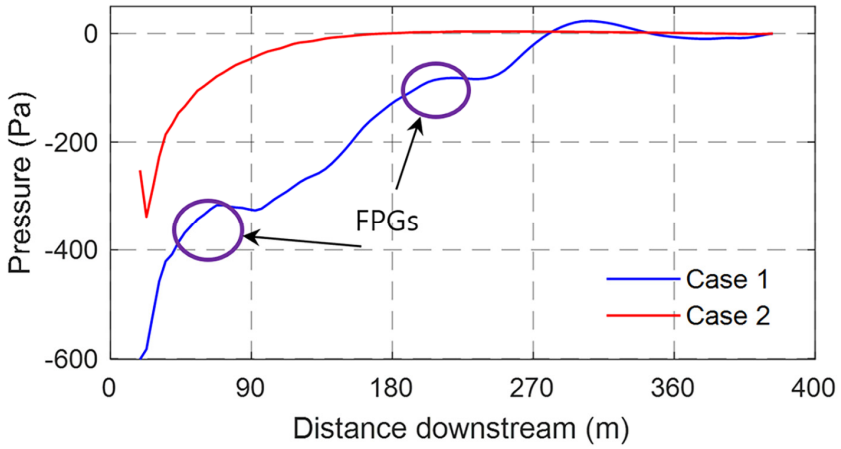

Fig. 13 Streamwise mean pressure distribution in the wake-recovery zone behind the turbine showing the existence of favorable and adverse pressure gradients

4. Conclusions

The focus of this study was to investigate and expand the knowledge of bathymetry-induced effects on turbine performance and wake behavior. The wake profile, vertical velocity distribution profile, and wake recovery were investigated. The impact on turbine torque and thrust was also assessed. Based on the results, the main conclusions of this study can be summarized as follows:

The presence of irregular bathymetry has a significant effect on the turbine wake. Flow is accelerated towards hill and ridge-like features owing to FPGs, causing a faster wake recovery (4.1% increase, compared to the flatbed case in this study). However, the presence of a slope-like feature creates an APG that decelerates the flow and, therefore, a slower wake recovery (11.1% reduction compared to the flatbed case in this study). Understanding the wake–bathymetry interaction effects is important for determining the optimal turbine location, especially when designing a tidal array farm.

The seabed feature can improve the turbine performance if located on a raised ridge-like feature (1.84% improvement compared to the flatbed case in this study). However, this may also result in an increased and highly fluctuating blade loading. Further research on bathymetry-induced loads on turbines is recommended for future studies.

Conflict of Interest

No potential conflict of interest relevant to this article was reported

Funding

This work was supported by a Grant-in-Aid for Early-Career Scientists (24K17456) from the Japan Society for the Promotion of Science, and by the Royal Society of Edinburgh 2023 Scottish Government SAPHIRE Grant award (ID: 3959).

References

Allmark, M., Ellis, R., Ebdon, T., Lloyd, C., Ordonez-Sanchez, S., Martinez, R., Mason-Jones, A ., Johnstone, C., & O'Doherty, T. (2021). A detailed study of tidal turbine power production and dynamic loading under grid generated turbulence and turbine wake operation. *Renewable Energy, 169*, 1422-1439. https://doi.org/10.1016/j.renene.2020.12.052

Allmark, M., Ellis, R., Lloyd, C., Ordonez-Sanchez, S., Johannesen, K., Byrne, C., Johnstone, C., O'Doherty, T., & Mason-Jones, A. (2020). The development, design and characterization of a scale model Horizontal Axis Tidal Turbine for dynamic load quantification. *Renewable Energy, 156*, 913–930. https://doi.org/10.1016/j.renene.2020.04.060

Allmark, M., Ordonez Sanchez, S., Wang, S., Kang, Y. S., Jo, C., O'Doherty, T., & Johnstone, C. (2019). An investigation into Reynolds scaling and solidity for a HATT tidal turbine. *Proceedings of the European Wave and Tidal Energy Conference 2019.*

Bir, G. S., Lawson, M. J., & Li, Y. (2011). Structural design of a horizontal-axis tidal current turbine composite blade. *Proceedings of the ASME 2011 30th International Conference on Ocean, Offshore and Arctic Engineering: Vol. 5. Ocean Space Utilization; Ocean Renewable Energy* (pp. 797–808). ASME. https://doi.org/10.1115/OMAE2011-50063

Brugger, P. A., Markfort, C., & Porte-Agel, F. (2022). Field measurements of wake meandering at a utility-scale wind turbine with nacelle-mounted Doppler lidars. *Wind Energy Science, 7*(1), 185–199. https://doi.org/10.5194/wes-7-185-2022

Chen, L., Wang, H., Yao, Y., Zhang, Y., & Li J. (2023). Experimental investigation of the seabed topography effects on tidal stream turbine behavior and wake characteristics. *Ocean Engineering, 281*, 114682. https://doi.org/10.1016/j.oceaneng.2023.114682

Garcia-Novo, P., Inubuse, M., Matsuno, T., Kyozuka, Y., Archer, P., Matsuo, H., Henzan, K., & Sakaguchi, D. (2024). Characterization of the wake generated downstream of a MW-scale tidal turbine in Naru Strait, Japan, based on vessel-mounted ADCP data. *Energy, 299*, 131453. https://doi.org/10.1016/j.energy.2024.131453

Garcia-Novo, P., Kyozuka, Y., & Matsuo, H. (2018). Tidal energy resource assessment map for Nagasaki Prefecture. in *Proceedings of Grand Renewable Energy 2018*. https://doi.org/10.24752/gre.1.0_237

Gaurier, B., Ikhennicheu, M., Germain, G., & Druault, P. (2020). Experimental study of bathymetry generated turbulence on tidal turbine behaviour. *Renewable Energy, 156*, 1158–1170. https://doi.org/10.1016/j.renene.2020.04.102

Holmedal, L. E., Johari, J., & Myrhaug, D. (2013). The seabed boundary layer beneath waves opposing and following a current. *Continental Shelf Research, 65*, 27–44. https://doi.org/10.1016/j.csr.2013.06.004

Hurubi, S., Stallard, T., Stansby, P., Mullings, H., & Ouro, P. (2023). Characterization of turbulent flow and the wake of a tidal stream turbine in proximity to a ridge. *Proceedings of the European Wave and Tidal Energy Conference 2023. https://doi.org/10.36688/ewtec-2023-464*

Ikhennicheu, M., Germain, G., Druault, P., & Gaurier, B. (2019). Experimental investigation of the turbulent wake past real seabed elements for velocity variations characterization in the water column. *International Journal of Heat and Fluid Flow, 78*, 108426. https://doi.org/10.1016/j.ijheatfluidflow.2019.108426

Jump, E., Macleod, A., & Wills, T. (2020). Review of tidal turbine wake modelling methods: State of the art. *International Marine Energy Journal, 3*(2), 91–100. https://doi.org/10.36688/imej.3.91-100

Khare, V., & Bhuiyan, M. A., (2022) Tidal energy-path towards sustainable energy: A technical review. *Cleaner Energy Systems*,

3, 100041. https://doi.org/10.1016/j.cles.2022.10004

Launder, B. E., & Spalding, D. B. (1974). The numerical computation of turbulent flows. *Computer Methos in Applied Mechanics and Engineering, 3*(2), 269–289. https://doi.org/10.1016/0045-7825(74)90029-2

Mercier, P., & Guillou, S. (2021). The impact of the seabed morphology on turbulence generation in a strong tidal stream. *Physics of Fluids*, *33*(5), 055125. https://doi.org/10.1063/5.0047791

Mercier, P., Grondeau, M., Guillou, S., Thiebot, J., Poizot, E. (2020). Numerical study of the turbulent eddies generated by the seabed roughness. Case study at a tidal power site. *Applied Ocean Research, 97*, 102082. https://doi.org/10.1016/j.apor.2020.102082

Ministry of Environment, Government of Japan. (n.d.). *Tidal current survey data: Naruseto bathymetry map.* https://www.env.go.jp/content/900448221.pdf

Mwero, N., Fu, S., Inamitsu, T., Oyunge, B., Ordonez-Sanchez, S., Garcia-Novo, P., Johnstone, C., & Sakaguchi., D. (2024). Investigation of the effects of irregular bathymetry on the performance and eake vharacteristics of a tidal dtream turbine; a case study of a tidal power site. *Proceedings of 7th Asian Offshore Wind, Wave and Tidal Energy Conference Series (AWTEC2024)*, p. 10.

Ordonez-Sanchez, S., Allmark, M., Porter, K., Ellis, R., Lloyd, C., Santic, I., O'Doherty, T., & Johnstone, C. (2019). Analysis of a horizontal-axis tidal turbine performance in the presence of regular and irregular waves using two control strategies. *Energies, 12*(3), 367. https://doi.org/10.3390/en12030367

Ouro, P., & Nishino, T. (2021) Performance and wake characteristics of tidal turbines in an infinitely large array. *Journal of Fluid Mechanics, 925*, A30. https://doi.org/10.1017/jfm.2021.692

Ouro, P., & Stoesser, T. (2019). Impact of environmental turbulence on the performance and loadings of a tidal stream turbine. *Flow, Turbulence and Combustion,* 102, 613–639. https://doi.org/10.1007/s10494-018-9975-6

Ouro, P., Stansby, P., Macleod, A., Stallard, T., & Mullings, H. (2023). High-fidelity modelling of a six-turbine tidal array in the Shetlands. *Proceedings of the European Wave and Tidal Energy Conference 2023*. https://doi.org/10.36688/ewtec-2023-442

Ozawa, A., Tsani, T., & Kudoh, Y. (2022). Japan's pathways to achieve carbon neutrality by 2050–Scenario analysis using an energy modeling methodology. *Renewable and Sustainable Energy Reviews,* 169, 112943. https://doi.org/10.1016/j.rser.2022.112943

Waldman, S., Yamaguchi, S., O'hara Murray, R., & Woolf, D. (2017). Tidal resource and interactions between multiple channels in the Goto Islands, Japan. *International Journal of Marine Energy, 19*, 332–344. https://doi.org/10.1016/j.ijome.2017.09.002

Yan, Y., Xu, S., Liu, C., Zhang, X., Chen, J., Zhang, Z., & Dong, Y. (2022). Research on the hydrodynamic performance of a horizontal-axis tidal current turbine with symmetrical airfoil blades based on swept-back models. *Journal of Marine Science and Engineering, 10*(10), 1515. https://doi.org/10.3390/jmse10101515

Author ORCIDs

Author name	ORCID
Mwero, Ngome	0009-0001-6626-571X
Fu, Song	0000-0003-0121-9154
Inamitsu, Takafumi	0009-0000-6092-6989
Ordonez-Sanchez, Stephanie	0000-0002-7253-6299
Mwangi, Benson	0009-0005-8592-3828
Garcia-Novo, Patxi	0000-0002-4041-9055
Johnstone, Cameron	0000-0001-5171-1230
Sakaguchi, Daisaku	0009-0001-2067-5414